Science Bulletin xxx (xxxx) xxx

Contents lists available at ScienceDirect

Science Bulletin

journal homepage: www.elsevier.com/locate/scib

Short Communication

Wideband and low sidelobe graphene antenna array for 5G applications

Rongguo Song [a,b], Zhe Wang [b,c], Haoran Zu [d], Qiang Chen [b], Boyang Mao [e], Zhi Peng Wu [a,b], Daping He [b,c,*]

[a] School of Information Engineering, Wuhan University of Technology, Wuhan 430070, China
[b] Hubei Engineering Research Center of RF-Microwave Technology and Application, Wuhan University of Technology, Wuhan 430070, China
[c] State Key Laboratory of Silicate Materials for Architectures, Wuhan University of Technology, Wuhan 430070, China
[d] the National Key Laboratory of Antennas and Microwave Technology, Xidian University, Xi'an 710071, China
[e] Chongqing 2D Materials Institute, Liangjiang New Area, Chongqing 400714, China

ARTICLE INFO

Article history:
Received 5 July 2020
Received in revised form 10 August 2020
Accepted 10 September 2020
Available online xxxx

The upcoming fifth-generation (5G) mobile communication with low-latency, high-speed and high-data-capacity [1] can realize innovative services such as remote intelligent medical care, smart cities, Internet of Vehicles, and ultra-high-definition video [2,3]. Compared with current mobile communications, 5G services require a 5G network with 1000 times the capacity and 10–100 times the data transmission rate [4]. 5G communication can also realize large-scale connections between people and machines [5]. It will be the era of Internet of Everything. The realization of the interconnection of all things is essentially the communication between the transmitting antenna and the receiving antenna.

Proposed in the 5G antenna white paper released by Huawei in 2019 (5G Antenna White Paper New 5G, New Antenna. https://carrier.huawei.com/~/media/CNBGV2/download/products/antenna/New-5G-New-Antenna-5G-Antenna-White-Paper-v2.pdf), 5G antennas design requires all-band configuration, precise beam coverage, multi-user beamforming, radiation concentration and low loss. Additionally, to improve the data transmission rate and spectrum capacity, realize spectrum multiplexing and improve channel utilization, 5G antennas demands to have the properties of wideband and low side lobes. Meanwhile, with the popularization of wireless communication equipment, microwave frequency bands are becoming crowded, resulting in allocable bandwidth becoming narrower and narrower, this is one of the reasons for the decline in signal transmission rate. Therefore, the millimeter-wave communication with the advantages of rich spectrum resources, miniaturization, high directivity and high resolution has attracted the attention of researchers and experts [6]. In 2017, the MIIT released the millimeter wave working frequency band of the 5G system, which is 24.75–27.5 GHz [7]. As the frequency increases, the communication distance will shorten, and the coverage of the base station will be greatly reduced. In addition, device-to-device (D2D) is a key technology for 5G wireless communication. Thus, the demand for 5G antennas will increase significantly. Traditional metal antennas can obtain high gain, but there are still some deficiencies in light weight, fast thermal conduction, low cost, and related issues with e-waste management [8].

Graphene, known as the most magical material of the 21st century, has caused extensive research by scholars from all walks of life in recent years due to it exceptional properties. As the lightest material, graphene with excellent flexibility based on unique two-dimensional structure has exceptional electrical and thermal conductivity [9]. In addition, as a carbon material, graphene has better chemical stability and adaptability to complex environments than metals [10]. All the above properties are very attractive to electronic devices, especially the antennas in 5G mobile communications system. Recently, a flexible high conductivity graphene assembled film (GAF) was applied to antenna design reported in our previous works. The GAF antennas exhibited comparable gain, radiation patterns, and return loss to commercial copper antennas [11–13]. On this basis, we further investigate the development of GAF millimeter wave large antenna array.

Here, we presented a millimeter-wave antenna array with 128 elements based on GAF for 5G mobile communication, which shows gratifying wideband and low sidelobes performances. The GAF antenna array designed as Chebyshev current distribution operate at 25.92 GHz with the measured –10 dB impedance bandwidth from 24 to 27.82 GHz, which covers the 5G millimeter-wave communication band. The sidelobes of GAF antenna array radiation patterns are lower than –20 dB. The radiation patterns and gain of GAF antenna array are measured and presented similar performances to the copper counterparts. The proposed GAF wideband

* Corresponding author at: Hubei Engineering Research Center of RF-Microwave Technology and Application, Wuhan University of Technology, Wuhan 430070, China.
E-mail address: hedaping@whut.edu.cn (D. He).

https://doi.org/10.1016/j.scib.2020.09.028
2095-9273/

and low sidelobes millimeter-wave antenna array in this work reveal its valuable prospective in 5G mobile communication.

Fig. 1a is the digital photo of GAF, which indicates excellent durability and flexibility. The GAF is with high conductivity of 1.12×10^6 S/m, measure by four probe method. From scanning electron microscope (SEM) image (inset of Fig. 1a), it shows there are many micro-folds on the surface of GAF, which attributes to flexibility. The X-ray diffraction (XRD) pattern of the GAF in Fig. 1b shows that the characteristic graphitic peak locates at $2\theta = 26.5°$, which indicates that the GAF has a stacking of graphene

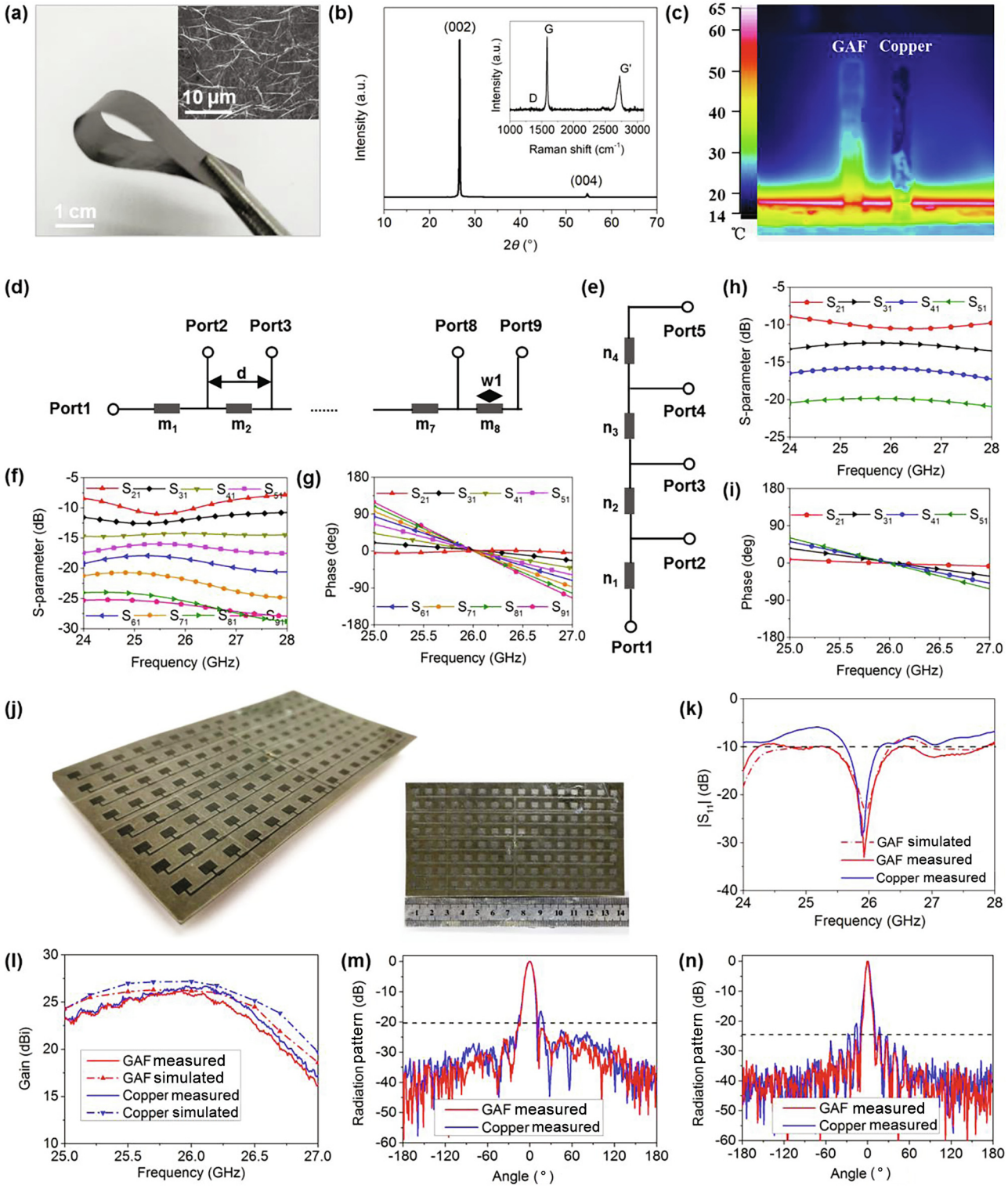

Fig. 1. (Color online) (a) Digital photograph and surface SEM image (illustration) of GAF. (b) XRD pattern and Raman spectra (inset) of GAF. (c) Thermal conduction comparison of GAF and copper. (d, e) Structure diagrams of HFN and VFN, respectively. The S-parameters and phases distribution of HFN (f, g) and VFN (h, i). (j) Digital photograph of GAF antenna array. (k, l) Simulated and measured reflection coefficients and gain. (m, n) Measured E-plane and H-plane radiation patterns of GAF antenna array and copper antenna array.

layers and with an interlayer spacing of ~0.34 nm. The strong intensity of the diffraction peak (004) indicates the GAF with a high degree of graphitization. The weak D band and strong G′ band of Raman spectra in the inset of Fig. 1b showing high quality graphitization after annealing process is also in agreement with XRD data. In Fig. S1 (online), a typical GAF film with a total thickness of ~26 μm and the density of 1.45 g/cm^3 possesses the structure of assembled stacking of graphene layers. Fig. 1c illustrates the infrared image of thermal conductivity contrast between GAF and copper foil. It can be seen that the GAF has much higher thermal conduction than copper foil, which has great benefits for high-power devices and antenna arrays.

Based on the advantages of GAF, we aim to achieve a wideband, narrow radiation beam and low sidelobes millimeter-wave microstrip antenna array. Fig. S2a (online) illustrates the structure of GAF microstrip antenna element which fed by the microstrip line embedded in the radiation patch. The dielectric substrate (blue part) is Rogers 5880 with thickness (h) of 0.508 mm and dielectric constant (ε_r) of 2.2. The physical dimensions of patch and microstrip line based on GAF are designed by the following formula [14].

$$L = \frac{c}{2f_{res}\sqrt{\varepsilon_{reff}}} - 2\Delta L, \tag{1}$$

$$W = \frac{c\sqrt{2}}{2f_{res}\sqrt{\varepsilon_r + 1}}, \tag{2}$$

$$\varepsilon_{reff} = \frac{\varepsilon_r + 1}{2} + \frac{\varepsilon_r - 1}{2}\left(1 + 12\frac{h}{W}\right)^{-1/2}, \tag{3}$$

$$\Delta L = 0.412h\frac{(\varepsilon_{reff} + 0.3)\left(\frac{W}{h} + 0.264\right)}{\varepsilon_{reff} - 0.258\left(\frac{W}{h} + 0.8\right)}, \tag{4}$$

$$Z_c = \begin{cases} \frac{60}{\sqrt{\varepsilon_e}}\ln\left[\frac{8h}{W_0} + \frac{W_0}{4h}\right] & \frac{W_0}{h} \leqslant 1 \\ \frac{120\pi}{\sqrt{\varepsilon_e}\left[\frac{W_0}{h} + 1.393 + 0.667\ln\left(\frac{W_0}{h} + 1.444\right)\right]} & \frac{W_0}{h} \geqslant 1 \end{cases}, \tag{5}$$

where L and W are the physical length and width of microstrip patch, respectively. Z_c is the characteristic impedance of microstrip feeder (with width of W_0). The structure is modelled and optimized in CST Studio. After parameters optimization, the length of the antenna element is L = 3.41 mm, the width is W = 4.35 mm, and the width of the microstrip line with the characteristic impedance of 100 Ω is W_0 = 0.44 mm. The GAF antenna element operates at 26 GHz with the −10 dB impedance bandwidth from 25.46 to 26.61 GHz, as illustrated in Fig. S2b (online). Fig. S2c, d (online) elucidate the radiation patterns of GAF antenna element. The half power beam width of E-plane and H-plane of GAF antenna array are 76.8° and 72.3°, respectively. The realized gain at 26 GHz is 7.3 dBi, which is suitable for antenna array design. The antenna array can effectively increase the gain and regulate the radiation beam width. A 16 × 8 GAF microstrip patch antenna array is proposed, as shown in Fig. S3 (online). The proposed GAF antenna array is fed in series and parallel with Chebyshev distribution. In the horizontal direction, a 1 × 16 line antenna array is symmetrical to the left and right, each of which has eight elements in series. In the center, a T-type power divider is used to feed the two sides of the line array in parallel. In the same way, in the vertical direction, there are four groups of line arrays in series at the top and bottom respectively, and the middle is fed in parallel by T-type power divider.

Due to the symmetry of the antenna array, only half of the horizontal feeding network (HFN) and vertical feeding network (VFN) need to be designed. Fig. 1d illustrates the structure diagram of HFN. Port 1 is the feeding port, and ports 2–9 are the radiation ports. In order to ensure that each radiation patch has the same excitation phase to resultant the normal radiation direction, the spacing (d) between the adjacent antenna elements is λ_g (λ_g is the waveguide wavelength). There is a quarter wavelength impedance converter (QWC, m_1–m_8, $w1$ = 1/4 λ_g) in front of each array element, which can realize the impedance matching of the feeding network. In addition, adjusting the characteristic impedance by changing the widths of each QWC can control the power distribution between each antenna element. The detailed parameters of QWC width are shown in Table S1 (online). Like HFN, the structure diagram of VFN is depicted in Fig. 1e. n1–n4 are the QWC in VFN, and the details are also shown in Table S1. The input power of each radiation port satisfies the Chebyshev distribution and has the same phase at 26 GHz, as demonstrated in Fig. 1f, g (HFN) and Fig. 1h, i (VFN).

The surface electric field distribution can clarify the radiation state of the antenna array. It can be seen from Fig. S4a (online) that the electric field distribution of GAF antenna array presents central symmetry, the electric field intensity is the strongest at the middle feeding end, and it becomes weak at the edge, which conforms to Chebyshev distribution. In addition, the electric field on 128 antenna elements is symmetrically distributed on the radiation edge, which indicates that GAF antenna array is in a good radiation state. Voltage Standing Wave Ratio (VSWR) represents the impedance matching of antenna system and is an important technical indicator of antenna array. Fig. S4b (online) shows the simulated VSWR of GAF antenna array is less than 2 in the range of 24–27.96 GHz (except 26.43–26.87 GHz), with a minimum of 1.14 at 26 GHz. To further investigate the radiation performance, the three dimensional (3D), normalized E-plane and H-plane radiation patterns of GAF antenna array are simulated as shown in Fig. S4c–e (online). The half power beam width of E-plane and H-plane of GAF antenna array is 10.3° and 5.1° with the sidelobes level is −23.67 and −24.65 dB, respectively.

The proposed GAF antenna array with the geometrical dimensions of 145 mm × 75 mm × 0.54 mm is fabricated using laser engraving method, as shown in Fig. 1j. For comparison, a copper antenna array with the same structure and size is fabricated and measured (Fig. S5 online). Fig. 1k depicts the reflection coefficients of the GAF and copper antenna array. The measured central frequency of the GAF antenna array by PNA (Keysight N5247A) is 25.92 GHz with the return loss of 33.02 dB, which is consistent with the simulated result. It is worth noting that the measured −10 dB impedance bandwidth of GAF antenna array is 14.7% (3.82 GHz) covering the range from 24 to 27.82 GHz, which is six times of that of copper antenna array (25.62–26.18 GHz). Wideband characteristic benefits from the lower Q value of GAF antenna array.

The gain of the GAF and copper antenna array are simulated and measured, as illustrated in Fig. 1l. In the bandwidth range of 25–27 GHz, the average gain of GAF antenna array is 21.81 dBi with the characteristic value of 25.68 dBi. Compared with copper antenna array, GAF antenna array only has a gain loss of 3.1% (0.8 dBi), which is acceptable in antenna array design. In addition, the E-plane and H-plane radiation patterns of GAF and copper antenna array are measured in anechoic chamber, as displayed in Fig. 1m, n and Fig. S6 (online). GAF and copper antenna arrays have the same main radiation direction and half power beam width. The half power beam width of GAF antenna array in E-plane and H-plane are 10.4° and 5.2°, respectively, which are narrower than the antenna element radiation beam. Interestingly, the sidelobes level of GAF antenna array is below −20 dB, which is lower than the copper antenna array.

In conclusion, a wideband and low sidelobes millimeter-wave antenna array based on high electrical and thermal conductivity graphene assembled film is presented. As a result, the designed GAF antenna array works at 26 GHz, a millimeter wave band of

5G mobile communication, has been proposed and investigated for the first time. The GAF antenna array also has similar radiation patterns and realized gain compare to the copper antenna array. Moreover, compared with copper antenna array, GAF antenna array has better working bandwidth (6 times of copper antenna array) and lower side lobe. Therefore, GAF antenna array is more suitable for 5G mobile communication antenna design.

Conflict of interest

The authors declare that they have no conflict of interest.

Acknowledgments

This work was supported by the National Natural Science Foundation of China (51701146 and 51672204), the Foundation of National Key Laboratory on Electromagnetic Environment Effects (614220504030617), and the Fundamental Research Funds for the Central Universities (WUT: 2020-YB-032, 205209016 and 2019IB017).

Author contributions

The manuscript was written through the contributions of all authors. Rongguo Song and Daping He had consideration for the idea and designed the experiments. Boyang Mao, Zhipeng Wu and Daping He oversaw the project progress. Rongguo Song, Zhe Wang and Qiang Chen performed the main experiments and analyzed the data. Rongguo Song, Boyang Mao, Zhe Wang and Daping He wrote the manuscript.

Appendix A. Supplementary materials

Supplementary materials to this article can be found online at https://doi.org/10.1016/j.scib.2020.09.028.

References

[1] Ohlen P, Skubic B, Rostami A, et al. Data plane and control architectures for 5G transport networks. J Lightwave Technol 2016;34:1501–8.
[2] Rao SK, Prasad R. Impact of 5G technologies on smart city implementation. Wireless Pers Commun 2018;100:161–76.
[3] Médard M. Is 5 just what comes after 4?. Nat Electron 2020;3:2–4.
[4] Ijaz A, Zhang L, Grau M, et al. Enabling massive IoT in 5G and beyond systems: PHY radio frame design considerations. IEEE Access 2016;4:3322–39.
[5] Ilderem V. The technology underpinning 5G. Nat Electron 2020;3:5–6.
[6] Tamayo-Dominguez A, Fernandez-Gonzalez J-M, Castaner MS. Low-cost millimeter-wave antenna with simultaneous sum and difference patterns for 5G point-to-point communications. IEEE Commun Mag 2018;56:28–34.
[7] Mao C-X, Khalily M, Xiao P, et al. Planar sub-millimeter-wave array antenna with enhanced gain and reduced sidelobes for 5G broadcast applications. IEEE Trans Antennas Propagat 2019;67:160–8.
[8] Awasthi AK, Li J, Koh L, et al. Circular economy and electronic waste. Nat Electron 2019;2:86–9.
[9] Xin G, Yao T, Sun H, et al. Highly thermally conductive and mechanically strong graphene fibers. Science 2015;349:1083–7.
[10] Zhang N, Wang Z, Song R, et al. Flexible and transparent graphene/silver-nanowires composite film for high electromagnetic interference shielding effectiveness. Sci Bull 2019;64:540–6.
[11] Song R, Zhao X, Wang Z, et al. Sandwiched graphene clad laminate: a binder-free flexible printed circuit board for 5G antenna application. Adv Eng Mater 2020. https://doi.org/10.1002/adem.202000451.
[12] Song R, Wang Q, Mao B, et al. Flexible graphite films with high conductivity for radio-frequency antennas. Carbon 2018;130:164–9.
[13] Zhang J, Song R, Zhao X, et al. Flexible graphene-assembled film-based antenna for wireless wearable sensor with miniaturized size and high sensitivity. ACS Omega 2020;5:12937–43.
[14] Song R, Huang G-L, Liu C, et al. High-conductive graphene film based antenna array for 5G mobile communications. Int J RF Microw Comput Aided Eng 2019;29:e21692.

Rongguo Song received Master of Science degree from School of Science, Wuhan university of Technology in 2018. He is currently pursusing Ph.D. degree in the Hubei Engineering Research Center of RF-Microwave Technology and Application, Wuhan University of Technology. His research interest includes graphene based materails, RF and microwave devices design.

Daping He is a full professor at Wuhan University of Technology (WUT). He obtained his Ph.D. degree in Materials Processing Engineering from WUT in 2013. He was a postdoctoral fellow in the University of Science and Technology of China. Then he joined University of Bath as a Newton International Fellow and University of Cambridge as a postdoctoral fellow. His research interest is preparation and application of nano-composite materials into new energy devices, sensors and RF microwaves field.